ARCHIVIO ISTITUZIONALE DELLA RICERCA

Alma Mater Studiorum Università di Bologna
Archivio istituzionale della ricerca

Optimal Management of Reversible Heat Pump/Organic Rankine Cycle Carnot Batteries

This is the final peer-reviewed author's accepted manuscript (postprint) of the following publication:

Published Version:
Torricelli N., Branchini L., De Pascale A., Dumont O., Lemort V. (2023). Optimal Management of Reversible Heat Pump/Organic Rankine Cycle Carnot Batteries. JOURNAL OF ENGINEERING FOR GAS TURBINES AND POWER, 145(4), 1-10 [10.1115/1.4055708].

Availability:
This version is available at: https://hdl.handle.net/11585/926860 since: 2024-06-04

Published:

DOI: http://doi.org/10.1115/1.4055708

Terms of use:

Some rights reserved. The terms and conditions for the reuse of this version of the manuscript are specified in the publishing policy. For all terms of use and more information see the publisher's website.

This item was downloaded from IRIS Università di Bologna (https://cris.unibo.it/).
When citing, please refer to the published version.

(Article begins on next page)

17 September 2026

American Society of Mechanical Engineers

ASME Accepted Manuscript Repository

Institutional Repository Cover Sheet

First Last

ASME Paper Title: Optimal Management of Reversible Heat Pump/Organic Rankine Cycle Carnot Batteries

Authors: Torricelli N.; Branchini L.; De Pascale A.

ASME Journal Title: JOURNAL OF ENGINEERING FOR GAS TURBINES AND POWER

Volume/Issue 145:4 Date of Publication (VOR* Online) 01 Apr 2023

ASME Digital Collection URL: https://asmedigitalcollection.asme.org/gasturbinespower/article/145/4/041010/1146 Management-of-Reversible-Heat-Pump-Organic

DOI: https://dx.doi.org/10.1115/1.4055708

*VOR (version of record)

OPTIMAL MANAGEMENT OF REVERSIBLE HEAT PUMP/ORC CARNOT BATTERIES

Noemi Torricelli
University of Bologna
Bologna, IT

Lisa Branchini
University of Bologna
Bologna, IT

Andrea De Pascale
University of Bologna
Bologna, IT

Olivier Dumont
University of Liège
Liège, BE

Vincent Lemort
University of Liège
Liège, BE

ABSTRACT

In the view of reducing the global greenhouse gas emissions it becomes fundamental to exploit the renewable energy sources at their maximum potential by developing effective strategies for their flexible use. Among the available solutions to realize these strategies are the electric energy storages including the innovative Pumped Thermal Energy Storage technology (included in the Carnot battery concept). This can become very interesting in these applications where different energy flows must be handled (both electric and thermal), thanks to the possibility of adding the contribution of a waste heat source, in a thermally integrated energy storage. However, despite the several advantages, the state-of-the-art still lacks experiments and investigation of efficient control strategy for the Carnot battery when inserted into the process. As original contribution to the current literature, this paper presents the off-design model of a reversible Organic Rankine Cycle (ORC)/Heat Pump (HP) Carnot battery configuration with the aim of employing it to simulate the performance of such system and discuss its optimal management when inserted into a generic process. An existing reversible HP/ORC kW-size prototype is considered as reference and its optimal control in both HP and ORC mode under different boundary conditions is assessed.

Keywords: Carnot Battery, Pumped Thermal Energy Storage, reversible ORC, energy storage, optimal control

NOMENCLATURE

Acronyms

CB	Carnot Battery
COP	Coefficient Of Performance
DH	District Heating
HP	Heat Pump
ORC	Organic Rankine Cycle
PV	Photovoltaic panels
ul	Upper Limit
WH	Waste heat

Abbreviations

aux	Auxiliary
ava	Available
comp	Compressor
dem	Demand
exp	Expander
nom	Nominal
opt	Optimal
PP	Pump
pur	Purchase
ren	Renewable
sub	Substation
sto	Storage

Symbols

A	Surface area (m^2)
C	Energy price (€/Wh)
ΔC	Differential cost (€)
E	Energy (Wh)
$\dot{m}$	Mass flow rate (kg/s)
$\dot{Q}$	Thermal power (W)
P	Pressure (Pa)
T	Temperature (°C)
$\dot{V}$	Volume flow rate (m^3/s)
V	Volume (m^3)
$\dot{W}$	Electrical power (W)
η	Efficiency (-)
ρ	Density (kg/m^3)

1 INTRODUCTION

Reducing the greenhouse gas emissions is one of the greatest challenges of our time. Among the means which can help to achieve the feat is the ever-increasing use of renewable energy sources. However, when a renewable energy system is integrated with an industrial process, in order to fully exploit its potential, it becomes necessary to develop strategies for the flexible use of renewable energies able to limit the mismatch between the production and the process demand. A well-known solution relies on the use of electrical energy storages, which nevertheless can be realized by means of different technologies, e.g. pumped hydro-storage, reversible fuel cells combined with hydrogen storage, batteries (and redox flow batteries), compressed air energy storage, liquid air energy storage, gravity energy storage.

Among energy storage typologies, none is prevailing, since the choice of one rather than another should account for several factors, depending on the application, and the research of performant solutions is still ongoing. In this context, the innovative Pumped Thermal Energy Storage technology (included in the Carnot battery concept) becomes interesting if compared to the others, due to its long cycle life, no geographical limitations, no need of fossil fuel streams and capability of being integrated into conventional fossil-fueled power plants or with any other type of waste heat source [1].

There are different configurations of Carnot batteries, characterized by different heating technologies to charge and discharge the thermal energy storage. The Carnot battery allows the storage of the surplus electric energy by converting it into heat (in HP mode) and then reconverting it back into electric energy (in ORC mode) when needed. Among the different options there is the reversible heat pump HP/ORC power system. In this configuration, the HP and the ORC system are embodied in a single and compact power plant, in which the ORC and the HP share the same volumetric machines, the same heat exchangers and the same working fluid. This system, in particular, can become very interesting in these applications where different energy flows must be handled (both electric and thermal), thanks to the possibility of adding the contribution of a waste heat source, in a thermally integrated energy storage. Indeed, when an external heat source is present, the heat pump can be employed with a low lift (high COP) [2] to increase the heat source temperature with the aim of increasing the ORC efficiency, which will work under higher temperature difference. In this context, interesting sectors of application are for example the data center, stationary engine, industries, district heating networks, supermarkets and Net Zero Energy Buildings [1].

However, the reversible HP/ORC Carnot battery technology has not yet reached the technological maturity and relevance in the market. The state-of-the-art lacks prototypes demonstrating the performance and the reliability of the system and the storage technology should be also deeper investigated to find out the best solution which is a compromise between performance, cost and compactness [3]. In order to manage different energy flows, it is also fundamental to develop an efficient control strategy for the Carnot battery when inserted into the process. At the present day, analyzing the state of the art of the technology, very few studies are dedicated to this topic. On the design aspect, it can be cited the work of Eppinger et al. [4], discussing the role of the storage temperature and the storage lift, and of Fan et al. [5] analyzing the performance of the cycle in different configurations. On the experimental point of view, Dumont et al. investigated a reversible ORC/HP unit designed to be coupled with a passive house [6]. The same authors presented in [7] a part-load model of reversible HP/ORC to analyze the part load performance of the system.

As original contribution to the current literature on the topic, this paper presents the off-design model of a reversible ORC/HP Carnot battery configuration with the aim of employing it to simulate the performance of such system and discuss its optimal management when inserted into a possible process. To this purpose, an existing reversible HP/ORC kW-size prototype [8] is considered as reference and the available experimental data are used for the model calibration. The performances of the separated HP and ORC systems are obtained as function of the most influencing boundary conditions and control variables. An optimal control strategy is then developed accounting for the HP/ORC performance, with the aim of achieving the best possible performance of the whole system under variable process conditions and the maximum economic gain from the Carnot battery operation.

The document is organized as follow: section 2 describes the simulated system, comprising the Carnot battery and the process in which it is inserted; section 3 presents the optimization problem; section 4 presents the reversible ORC/HP system model and the implemented optimal management strategy; section 5 discusses the results; the conclusion section summarizes the contribution and the findings of the present work.

2 THE ENERGY SYSTEM

2.1 The components

A possible Carnot battery application in its most generic configuration comprises the following elements (see Figure 1, where components are numbered according to the list below):

1. An on-site electric power and a thermal power user, which require to satisfy a certain power demand.
2. An on-site renewable energy power plant, which can provide part of the entire power demand or the entire power demand or a surplus power production, depending on the availability of the energy source. In case of surplus of power production, the exceeding energy can be sold to the grid or stored into the Carnot battery to be released later.
3. The electric grid, from which it is possible to purchase the necessary missing amount of power to entirely satisfy the power demand.
4. Possibly, an on-site thermal power free source, since in many industrial and tertiary applications is not uncommon to find processes including a waste heat release [9]. In these cases, the available thermal power can be recovered to exercise the heat pump with a better COP and increase the ORC mode power production (in a thermally integrated configuration). The input thermal power can also come from a district heating or solar thermal panels where the retrieved energy presents a given cost.
5. The Carnot battery, which can be charged exploiting the renewable energy power plant production and the waste heat, and discharged to cover both the electric and the thermal user demand when requested. The ORC electrical production could also be sold to the grid when in excess.

In the case study, the Carnot battery is composed by the reversible HP/ORC prototype (described in the following paragraph) and a water tank, which serves as sensible thermal energy storage (see the Carnot battery detail in Figure 1). The hot storage represents the hot sink of the energy system, whilst the cold source consists in tap water. When the Carnot battery works in HP mode, in case the waste heat temperature (T_{WH}) is lower than the storage temperature (T_{sto}), the waste heat flow is used as HP cold source in place of the tap water, in order to enhance the HP performance.

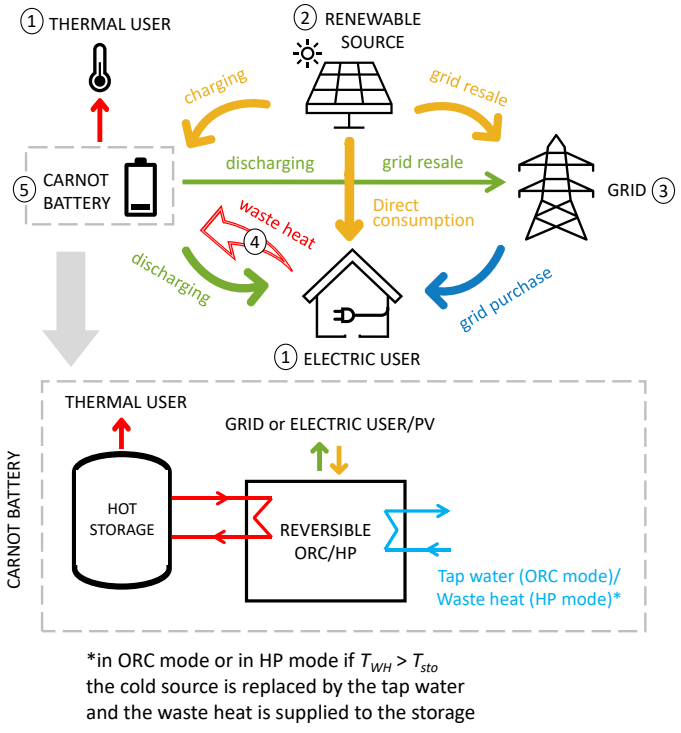

FIGURE 1: CARNOT BATTERY INTEGRATION INTO A GENERIC APPLICATION – POWER FLOWS.

2.2 The reversible ORC/HP prototype

The considerations made in this paper take as reference the reversible HP/ORC prototype installed at the University of Liège briefly presented here (for further information the reader is invited to consult the dedicated

experimental work [8]). The hydraulic scheme comprehending all the components and sensors is illustrated in Figure 2. The green loop is the main one; it is the refrigerant loop composed of a high-pressure (HP) heat exchanger, a scroll volumetric machine able to work as a compressor or as an expander, a low-pressure (LP) heat exchanger, and two parallel branches with an expansion valve and a pump to work alternatively in heat pump (charging) mode and ORC (discharging) mode. The refrigerant circulates clockwise when working in ORC mode and counterclockwise in heat pump mode.

More in detail, the volumetric machine is a scroll compressor from the automotive industry, which has been modified to be able to work reversibly as an expander. The ORC pump is a plunger pump chosen for its high volumetric and isentropic efficiency. Regarding the expansion valve, a solenoid valve is used to adjust the compressor suction superheating in heat pump mode. The condenser and the evaporator are plate heat exchangers, sized to keep the pinch point below 2 K. More details on the components' size are reported in Table 1 collecting the parameters used for modelling the reversible ORC/HP system.

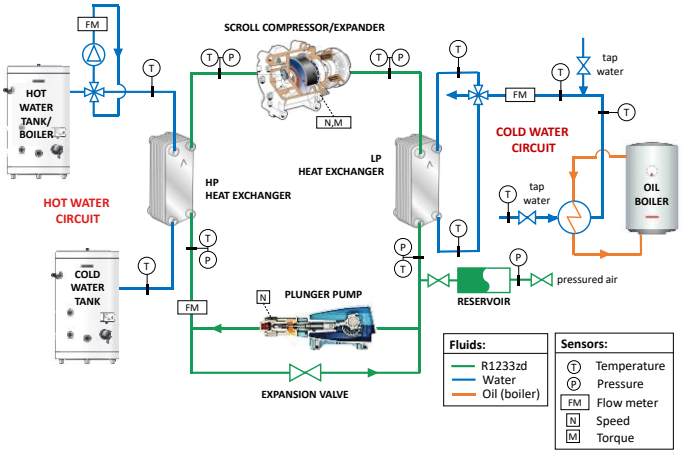

FIGURE 2: SCHEME OF THE REVERSIBLE CARNOT BATTERY BASED ON A REVERSIBLE HP/ORC UNIT.

The sizing of the prototype and the choice of the working fluid were achieved by assuming target boundary conditions representative of many industrial applications (i.e., ambient temperature equal to 15°C and waste heat temperature equal to 75°C), with the aim of obtaining an electrical production almost equal to the electrical consumption. In the design of the prototype, particular attention was paid to the Reynolds ratio parameter. The latter is defined as the ratio between the highest Reynolds number of the ORC mode and the highest Reynolds number in the HP mode, and should be set to about one in order to obtain similar working conditions and therefore good performance both in HP and ORC mode [10]. Under these assumptions, HFO-1233zd(E), with a critical temperature of 165 °C and a critical pressure of 35.7 bar, is chosen as high performant refrigerant. It is a non-flammable, ultra-low GWP (=4,5) born as replacement for R-123 for low pressure centrifugal chillers, which are most often used to cool large buildings [11].

In order to test the prototype under different boundary conditions, in term of hot and cold source temperature, the test bench is provided with other two external circuits (blue loops) where water circulates, simulating the hot and the cold source, feeding respectively the HP and the LP heat exchanger. The hot source loop presents two thermal energy storages in order to work with a perfect stratification between the hot zone and cold zone, where a pump provides the necessary flow to move the water from the hot water tank to the cold one in ORC mode and vice versa in HP mode by using a four-way valve. The same reversible layout is repeated for the cold source but no storage is present. In order to simulate different temperature levels, both the hot and the cold side are provided with an external heat source. The test-rig is then fully equipped with high accuracy sensors to determine the thermodynamic state of the fluids in each point of the cycle and the involved powers.

Experimental data collected on the rig are presented in [8] and are used for the calibration of some parameters of the reversible ORC/HP model, presented in section 4.1.

3 THE CARNOT BATTERY OPTIMAL MANAGEMENT

This section presents the problem implemented to determine the optimal Carnot battery management from the economic point of view, considering the energy system configuration presented in section 2.2 in case the waste heat is provided by a district heating substation. Section 3.1 presents the physical problem whilst section 3.2 describes the algorithm used to solve the problem.

3.1 Problem's description

The objective function is the economic benefit, as defined in Eq. (1), representing the differential cost between two scenarios, i.e., with and without the Carnot battery intervention.

The differential gain is equal to the sum of three positive gain contributions minus a cost contribution. The first two positive terms are associated to the gain obtained by the ORC energy production surplus ($E_{ORC,plus}$) sale and by the self-consumption of the ORC energy production ($E_{ORC,autocons}$), which leads to an avoided cost. The third one derives from the advantage of covering part of the thermal demand (and in particular the demand peaks) with the Carnot battery in place of alternatives energy systems. For instance, in case the thermal power demand was originally provided by a district heating network, installing a Carnot battery could allow for a different design of the substation (i.e., smaller size) with considerable reduction of the substation and piping investment cost.

Thus, the avoided cost would be proportional to Δsize_{sub} [kW], which represents the difference between the original substation size, and the new one, size_{sub}, resulting from the new design, considering the heat pump intervention. The proportionality constant is the fee, $C_{DH,fee}$ [€/kW] [16]. Since referred to the investment, this gain contribution must be split over the Carnot battery lifetime, $lifetime$, as indicated in Eq. (1). Finally, the cost contribution term is associated instead to the energy E_{HP}, which is provided to the HP, in place of being sold to the grid. Decisive parameters, which appear into Eq. (1), are the electric energy purchase cost, C_{pur}, and the electricity sale price, C_{sale}.

The ORC/HP power profiles, $\dot{W}_{ORC}$ and $\dot{W}_{HP}$, are optimization variables of the problem. The energy terms ($E_{ORC,plus}$, $E_{ORC,autocons}$ and E_{HP}), which appear in the objective function, derives from the integral of the Carnot battery produced/absorbed power (with the ORC/by the HP) over the considered time period, *T* (see Eq. (4)).

Objective:

$$\max\ \Delta C = \begin{matrix} E_{ORC,surplus} \cdot C_{sale} + E_{ORC,autocons} \cdot C_{pur} \\ + \Delta\text{size}_{sub} \cdot C_{DH,fee}/lifetime - E_{HP} \cdot C_{sale} \end{matrix} \quad (1)$$

Variables: $\dot{W}_{HP}$, $\dot{W}_{ORC}$ and $\dot{Q}_{CB2dem}$

Equations:

$$\dot{W}_{ORC,autocons,t} = \min\left(\dot{W}_{ORC,t}, \dot{W}_{dem,t}\right) \quad (2)$$

$$\dot{W}_{ORC,surplus,t} = \max\left(\dot{W}_{ORC,t} - \dot{W}_{dem,t}, 0\right) \quad (3)$$

$$E = \int_0^T \dot{W}\, dt \quad (4)$$

$$\dot{Q}_{DH2dem,t} = \dot{Q}_{dem,t} - \dot{Q}_{CB2dem,t} \quad (5)$$

$$\text{size}_{sub} = \max\left(\dot{Q}_{DH2dem}\right) \quad (6)$$

$$\dot{Q}_{HP,t} = COP_t\left(T_{sto,t}, \dot{W}_{HP,t}, T_{cold\ source,t}\right) \cdot \dot{W}_{HP,t} \quad (7)$$

$$\dot{Q}_{ORC,t} = \eta_t\left(T_{sto,t}, \dot{W}_{ORC,t}, T_{cold\ source,t}\right) \cdot \dot{W}_{ORC,t} \quad (8)$$

$$\frac{dT_{sto}}{dt} = \frac{\dot{Q}_{HP,t} - \dot{Q}_{ORC,t} - \dot{Q}_{CB2dem,t} - UA_{sto} \cdot \left(T_{sto,t} - T_{amb,t}\right)}{V_{sto} \cdot \rho \cdot c_p} \quad (9)$$

Constraints:

$$\dot{W}_{ORC,t} \in [0, \dot{W}_{min}: \dot{W}_{nom}] \quad (10)$$

$$\dot{W}_{HP,t} \in [0, \dot{W}_{min}: \min\left(\dot{W}_{nom}, \dot{W}_{ava,t}\right)] \quad (11)$$

$$\dot{Q}_{CB2dem,t} \in [0: \min\left(\dot{Q}_{CB,ava,t}, \dot{Q}_{dem,t}\right)] \quad (12)$$

The problem is a dynamic problem, since the optimal control strategy is called to decide the ORC/HP instantaneous load, which influence the storage conditions and the optimal management of the ORC/HP system in the next instants as a consequence. Indeed, the storage temperature, T_{sto}, can increase or decrease with the time, t, (as described in Eq. (9)) depending on: i) the HP/ORC system heat production/absorption ($\dot{Q}_{HP}/\dot{Q}_{ORC}$), determined by the HP/ORC operation; ii) the possible negative contribution of an external heat consumer ($\dot{Q}_{CB2dem}$), which can be an optimization variable; iii) and the heat losses contribution, $UA_{sto} \cdot (T_{sto} - T_{amb})$; where the storage inertia depends on the mass of fluid contained in the storage, $V_{sto} \cdot \rho$, and on its specific heat capacity, c_p.

The district heating is called to cover, $\dot{Q}_{DH2dem,t}$, i.e., the amount of the demanded power which cannot be satisfied by the Carnot battery with the $\dot{Q}_{CB2dem}$ contribution (see Eq. (5)). The new substation size, size$_{sub}$, will be equal to the maximum value taken by $\dot{Q}_{DH2dem}$ over the considered time period (see Eq. (6)). $\dot{Q}_{HP}$ and $\dot{Q}_{ORC}$ can be determined as function of the ORC/HP system electric absorbed/consumed power, $\dot{W}_{HP}$ /$\dot{W}_{ORC}$, when considering the HP or the ORC mode respectively (see Eqs. (7-8)). The relationship between $\dot{Q}_{HP}$ /$\dot{Q}_{ORC}$ and $\dot{W}_{HP}$ /$\dot{W}_{ORC}$ is expressed by means of the system efficiency, which varies not only with the boundary conditions (e.g. T_{sto}) but also with the controls operation (e.g. the pump/compressor speed influencing the organic fluid flow rate) which determine the system load (as further discussed in section 4). Thus, it must be noticed that in order to exercise the system at its maximum efficiency, under imposed boundary conditions and loads, it would be necessary to optimize the control variables. To this purpose an "optimal mode control strategy" should be implemented as part of the Carnot battery optimal management strategy. For more detail on the optimization variables, see section 4.2, describing the optimal ORC/HP management strategy implemented for the case study.

The constraints of the problem concern the ORC and HP operating limits related to the system maximum, $\dot{W}_{nom}$,and minimum technical load, $\dot{W}_{min}$, and the amount of renewable power in surplus, $\dot{W}_{ava,t}$, instantaneously available to run the Carnot battery in HP mode (see Eq. (10) and (11)). The ORC/HP power can also be null in case the ORC/HP reversible system is not called to work. The Carnot battery cannot work in ORC and HP mode simultaneously, thus the ORC and the HP power cannot be both higher than zero at the same time. $\dot{Q}_{CB2dem,t}$ is limited by the minimum value between the power stored into the Carnot battery, $\dot{Q}_{CB,ava,t}$ (available for the heat exchange, compatibly with the thermal user operating conditions) and the thermal user power demand, $\dot{Q}_{dem,t}$.

3.2 Optimization algorithm

The optimization problem is implemented in Maltab environment in all its parts. The algorithm solves the problem presented in section 3.1 by systematically evaluating the economic benefit (i.e. the objective function) for different combinations of HP/ORC power profiles. The combination which leads to the highest economic gain corresponds to the solution.

The Carnot battery operation is simulated time step by time step, following the routine in flowchart of Figure 3, for a given combination of ORC/HP upper limit power profiles, $\dot{W}_{HP,ul}/\dot{W}_{ORC,ul}$. It must be highlighted that $\dot{W}_{HP,ul}/\dot{W}_{ORC,ul}$ do not always correspond to the actual absorbed/produced power value, but rather to a first attempt. It is up to the optimal model control strategy to compute the actual value $\dot{W}_{HP}/\dot{W}_{ORC}$, respecting the process boundary conditions (see section 4.2). According to the flowchart, the algorithm evaluates the instantaneous process conditions to decide if turning on/off the Carnot battery and/or switching mode (ORC/HP). Five different situations may occur (indicated with number into circles in Figure 3):

- The demanded power, $\dot{W}_{dem}$, may be not entirely covered by the renewable energy source power plant production, $\dot{W}_{ren}$, resulting in a power deficit. In this case, the ORC operating limits (i.e., heat source temperature and technical minimum load) may be respected or not:
    1. if yes, the ORC is run according to the "optimal mode control strategy" (see section 4.2) producing the power $\dot{W}_{ORC}$ by discharging the thermal storage of an amount of power equal to $\dot{Q}_{ORC}$.
    2. if not, ORC is not run and the storage is not discharged. The storage temperature decreases anyway due to the heat losses to the ambient.
- $\dot{W}_{ren}$ may overcome $\dot{W}_{dem}$ resulting in a power surplus, $\dot{W}_{ava}$. In this case, the HP operating limits (i.e., heat source temperature and technical minimum load) may be respected or not:
    3. if yes, the HP is run according to the "optimal mode control strategy" (see section 4.2) absorbing the power $\dot{W}_{HP}$ to charge the storage of an amount of power equal to $\dot{Q}_{HP}$.

4. if not the, the HP is not run, the storage is not charged and the storage temperature slightly decreases due to the heat losses to the ambient.

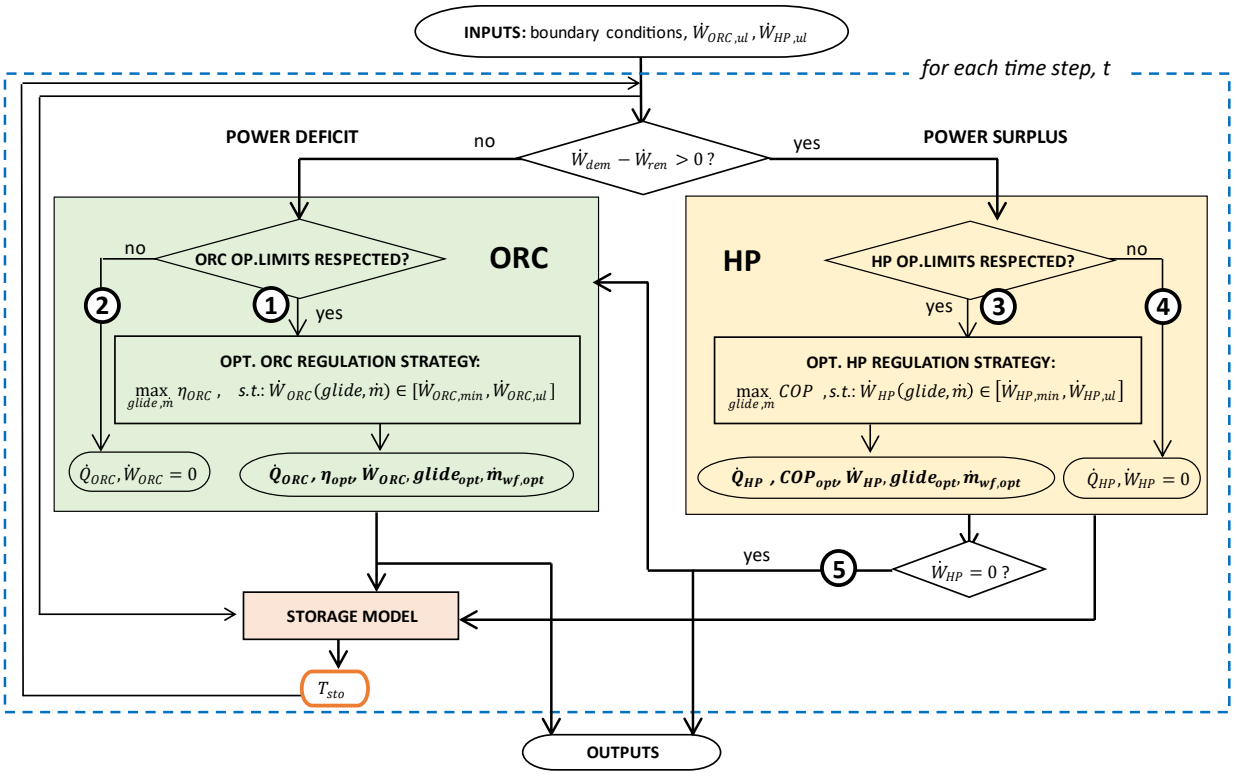

FIGURE 3: CARNOT BATTERY OPERATION FLOWCHART.

5. In case the HP is not called to work, the code tests the possibility of running the ORC to produce a power surplus to sell to the grid. This scenario could occur in case there is no electric demand to satisfy, but the Carnot battery is employed to maximize the electric energy sale and the related gain.

The boundary conditions (among which is T_{sto}) are assumed constant over the timestep interval and the ORC and HP operative conditions are assumed to be time-independent (which is a realistic assumption since the time constant of the storage is much larger than that of the ORC/HP). According to this hypothesis, the HP/ORC system works in steady-state operation during the timestep interval. The energy balance on the storage volume (see Eq. (9)) is discretized over the time step and implemented into the "STORAGE MODEL" block. The output of this block is the updated value of the storage temperature value, $T_{sto,t+t}$, for the successive timestep resolution, $t + 1$.

To cover the thermal user demand, it is assumed that the thermal storage is discharged only in correspondence of the demand peaks, and the discharged power profile, $\dot{Q}_{CB2dem}$, is the one that allow to minimize the district heating substation size, respecting the problem's constraints (see Eq. (12)). The routine is thus run iteratively, for each combination of the tested $\dot{W}_{HP,ul}/\dot{W}_{ORC,ul}$ profiles, in order to find the minimum possible substation size.

Once the Carnot battery operation is evaluated over the entire time period, the routine's outputs are the sequences of the actual HP/ORC instantaneous power values, the sum of which determines the energy outputs of the model, and the new substation size. On the basis of the resulting energy values, the economic gain is finally determined by means of Eq. (1), as the differential cost between two scenarios, i.e., with and without the Carnot battery intervention.

Respecting the problem's constraints, the HP power profile vectors are composed by power values limited between 0 and the power surplus available from the renewable source ($\dot{W}_{ava}$), whilst the ORC upper limit power profile vectors' elements can range between 0 and the ORC nominal power. In this way, different Carnot battery control strategies are indirectly tested, including different cases: i) HP and ORC exercised at maximum efficiency and maximum allowed power consumption/production, ii) renewable energy completely sold to the grid (i.e., HP off, the system would be equivalent to a classical ORC with a thermal storage), iii) variable charge and discharge times, obtained by operating the HP and the ORC at part-load, iv) combinations of the previous cases.

4 THE HP/ORC OPTIMAL MANAGEMENT

An optimal mode control strategy is implemented, as part of the optimization algorithm (see "OPT. HP/ORC CONTROL STRATEGY" in Figure 3), To this purpose, the ORC/HP model described in section 4.1 is used to map the ORC/HP performance and build lookup tables which allow to identify the maximum efficiency operation, under imposed boundary conditions.

4.1 ORC and HP models

The methodology used to model the ORC and the HP components is based on a semi-empirical approach for the off-design modelling of micro-ORCs, in line with the same method presented in [11]; more in detail:

The heat exchangers are modelled by means of the moving boundaries method [12]. A corrected version of the Cooper's (Eq. (13)) and the Gnielinski's (Eq. (14)) correlations is used to evaluate respectively the evaporating and the condensing convective heat transfer coefficients, as proved to be effective to simulate heat transfer in ORC applications [12]. The correction coefficients are here named as c_1, c_2 and c_3. The single phase regions convective heat transfer coefficient is determined instead by means of the Dittus-Boelter correlation [13].

$$h = c_1 \cdot \left(\frac{\dot{Q}}{A}\right)^{0.67 \cdot c_2} \cdot 55 \cdot P_r^{\,0.12 - 0.2 \cdot log P_r} \cdot -\log\left(P_r\right)^{-0.55 \cdot c_2} \cdot M^{-0.5} \qquad (13)$$

$$Nu = c_3 \cdot \frac{f/8 \cdot (Re - 1000) \cdot Pr}{1 + 12.7 \cdot (f/8)^{0.5} \cdot Pr^{2/3-1}} \qquad (14)$$

P_r indicates the reduced pressure, M, the molecular weight, Nu the Nusselt number and f the Darcy friction factor.

The scroll compressor/expander is modelled by means of the lumped parameter approach originally proposed by Lemort [14] for scroll compressors. Besides of under- and over-expansion/compression losses (due to the fixed built-in volume ratio of the machine), the model can account for pressure drops and heat transfers at the inlet and outlet ports of the machine, internal leakages, mechanical losses and heat losses to the environment.

The ORC pump model relies on Eq. (15) [15]. According to Eq. (15) the performance of the pump is influenced by its operating conditions in terms of rotational speed, N_{pp}, elaborated volume flow rate, $\dot{V}$, and pressure rise, ΔP. The performance depends also on the pump load and how much it deviates from the nominal point, represented by a nominal engine absorbed power, $\dot{W}_{eng,nom}$, rotational speed, $N_{pp,nom}$, and efficiency, $\eta_{eng,nom}$. The pump absorbed power is correlated to all these variables through the empirical parameters K_1, K_2, K_3 and K_4.

$$\dot{W}_{pp} = K_1 + K_2 N_{pp} + K_3 \dot{V} \Delta P + \dot{W}_{eng,nom}\left(\frac{1}{\eta_{eng,nom}} - 1\right) \cdot \left(K_4 \frac{(K_2 N_{pp} + K_3 \dot{V} \Delta P)^2}{\dot{W}_{eng,nom}^{\,2}} + (1 - K_4)\frac{N_{pp}^{\,2}}{N_{pp,nom}^{\,2}}\right) \qquad (15)$$

The HP expansion valve is represented by an isenthalpic expansion between the high (condensing) and the low (evaporating) pressure of the cycle. This assumption is verified during the experimental campaign [8].

The pressure drops are evaluated with Eq. (16), proportional to the square of the fluid mass flow rate, $\dot{m}_{wf}$, and to the flow coefficient, k [10].

$$\Delta P = k \cdot \dot{m}^{\,2} \qquad (16)$$

The auxiliary pumps consumption is also accounted using Eq. (17) and considering a constant efficiency. Where the auxiliary pumps are these pumps moving the fluid into the hot and cold external circuits, here called "secondary fluid".

$$\dot{W}_{aux} = \frac{\dot{V} \cdot \Delta P}{\eta_{pp,aux}} \qquad (17)$$

The inputs of the model represent the boundary conditions and the control variables of the system. The boundary conditions depend on the site and on the involved processes, and they are primarily the hot source and the cold source fluid state and the ambient temperature. The control variables are instead those variables which can be controlled by the outside, such as the secondary fluid temperature glide through the heat exchangers (i.e., the difference between the secondary fluid inlet and outlet temperature), the refrigerant flow rate, the superheating degree at the evaporator and the subcooling degree at the condenser. These variables are controlled respectively by regulating the cold and hot mass flow rates, the volumetric machine speed, the pump speed and the expansion valve opening. The latter are decisive parameters to adjust so as to achieve the best possible performance from the Carnot battery system for given boundary conditions.

Solving the problem via iterations over the cycle pressures, the part load model is able to evaluate as output: the fluid state in each point of the cycle, the thermal power exchanged into heat exchangers, the secondary fluids flow rate and the power consumed or produced by the machines. Other fundamental performance outputs that identify the Carnot battery performance are derived from Eqs. (18)-(19) and they are: the net power output ($\dot{W}_{net}$), the ORC net efficiency (η), the HP coefficient of performance (*COP*) where the thermal energy storage is assumed to be perfectly stratified and without ambient losses.

$$\dot{W}_{net,ORC} = \dot{W}_{exp} - \dot{W}_{pp} - \dot{W}_{aux} \mid \dot{W}_{net,HP} = \dot{W}_{comp} + \dot{W}_{aux} \quad (18)$$

$$\eta = \frac{\dot{W}_{net,ORC}}{\dot{Q}_{ev,ORC}} \mid COP = \frac{\dot{Q}_{cd,HP}}{\dot{W}_{net,HP}} \quad (19)$$

The semi-empirical model relies on the parameters, listed in Table 1, with their corresponding values. The parameters' calibration process is performed by fitting the experimental data such that to identify the parameters values that minimize the mean square error between the experimental and calculated values.

TABLE 1: MODELS' PARAMETERS.

Component	Parameter	Value
Pump (PP)	K_1 (W)	20
	K_2 (W·s)	0.07
	K_3 (-)	1.17
	K_4 (-)	0.6
Compressor (COMP)	Ambient heat losses (W/(m^2 K))	5
	Supply heat losses (W/(m^2 K))	10
	Exhaust heat losses (W/(m^2 K))	10
	Leakage area (m^2)	1e-8
	Mechanical constant losses (W)	10
	Swept volume(m^3)	3.8e-5
	Built in volume ratio (-)	2
	Exhaust pressure drop diameter (m)	0.0098
Expander (EXP)	Ambient heat losses (W/(m^2 K))	1
	Supply heat losses (W/(m^2 K))	50
	Exhaust heat losses (W/(m^2 K))	94
	Leakage area (m^2)	2.6e-6
	Mechanical proportional losses (-)	0.02
	Mechanical constant losses (W)	8
	Swept volume(m^3)	3.8e-5
	Built in volume ratio (-)	2.2
	Supply pressure drop diameter (m)	0.0098
High pressure Heat exchanger (HP-CD/ORC-EV)	Equivalent diameter (m)	0.02
	Surface (m^2)	2.52
	Cooper correlation coefficient, c_1 (-)	0.98
	Cooper correlation coefficient, c_2 (-)	1.08
Low pressure Heat exchanger (HP-EV/ORC-CD)	Equivalent diameter (m)	0.02
	Surface (m^2)	2.38
	Gnielinski correlation coefficient, c_3 (-)	4.62
aux pumps	Efficiency (%)	50

4.2 Optimal HP/ORC mode control strategy

For each combination of available hot source temperature (i.e., storage temperature), cold source temperature and produced/absorbed power (in ORC/HP mode, respectively), it exists an optimal value of the secondary fluid temperature glide (or more simply called "glide") and of the working fluid flow rate that maximize the system net efficiency (η or COP, see Eq. (19)) (as shown in [7]). It must be highlighted that the maximum efficiency point does not always correspond to the maximum power production, in ORC mode, and to the minimum power consumption, in HP mode [7].

In order to identify the optimal HP/ORC operation under given boundary conditions, an optimal control mode strategy is implemented into the "OPT. HP/ORC CONTROL STRATEGY" function, based on the interpolation of data contained into lookup tables, representing the system performance map, obtained by simulating the system in a wide range of operating conditions by means of the HP/ORC model presented above. Inputs to provide to the optimal control model function are: i) the storage temperature, ii) the upper limit value of the power demanded (or available) by the ORC (to the HP). The latter represents a constraint to not overcome; according to this constraint the maximum efficiency point is selected among the points at power production/consumption lower than the power upper limit value. Outputs of the function are the optimal working conditions in terms of glide, working fluid flow rate, efficiency, $\dot{Q}_{ORC}/\mathrm{Q}_{HP}$ and actually produced/consumed power, W_{ORC}/W_{HP} (see Figure 3).

For the case study, the performance maps have been created by assuming constant values of the superheating and the subcooling degree, both equal to 5 °C. In first instance, the evaporator and the condenser glides are considered equal, to limit the involved variables.

5 RESULTS AND DISCUSSION

Results of this work can be divided in 2 sections: i) "Optimal HP/ORC model control strategy maps", discussing the results of the application of the "Optimal mode control strategy model" in terms of HP and ORC performance; ii) "Carnot battery optimal management: a case study", presenting the results of the application of the "Optimal global control strategy" on a case study; analyzing the introduction of the Carnot battery in a process, its performance and its economic feasibility.

5.1 Optimal HP/ORC mode control maps

The results of the "optimal mode control strategy model" can be represented in form of the control maps of Figure 4, which graphically reproduce the data contained in the optimal control lookup tables. The empty areas correspond to not physically feasible operating points and represent the operating limits of the system.

For the ORC a possible operating range of temperature from 70 to 100 °C is considered, resulting in a maximum net power output of about 3 kW, when the cold source temperature is equal to 15 °C. The results show that the optimal ORC net efficiency increases with the temperature and the demanded power output, ranging between 6 and 9 %. In order to reach the maximum efficiency for each boundary conditions' combination:

- the working fluid mass flow rate must be almost linearly incremented with the demanded power output. Indeed, the power production is generally proportional to the mass flow rate, since the higher is the mass flow rate, the higher is the thermal power exchanged into the evaporator (and into the condenser) and the power available for the expansion process. However, the higher is the mass flow rate, the higher is also the pump consumption, which can strongly affect the ORC global performance.
- In most of the cases, instead, the glide must be incremented with the available hot source temperature. The glide influences in particular the pressures inside the cycle and, thus, the available cycle pressure ratio. This parameter is crucial since the more it differs from the machine built in pressure, the higher are the under-expansion and over-

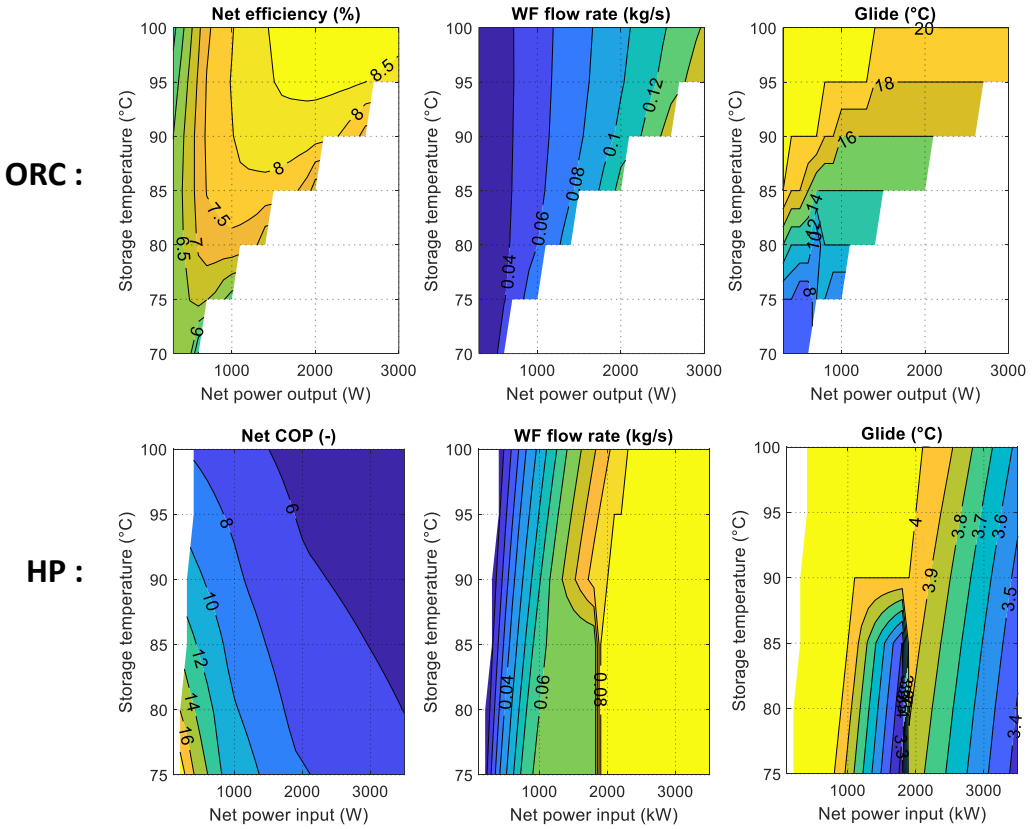

FIGURE 4: RESULTS OF THE ORC/HP MODE CONTROL STRATEGY.

expansion losses at the expander. This is why it is important to adjust it as function of the boundary conditions

(and in particular of the temperature levels) in order to achieve the best possible performance of system. Other aspects influenced by the glide are the secondary fluid pump consumption and the heat exchangers irreversibilities.

Concerning the HP, the hot source temperature lower and upper operating limits are set equal to 75 to 100 °C, when the cold source temperature is equal to 75 °C (considered as design operating point). The results show that the lower are the storage temperature (and thus, the temperature lift) and the absorbed power, the higher is the achievable total COP, which can reach a maximum value of 18. In order to reach the maximum COP for each boundary conditions' combination, the working fluid mass flow rate must be incremented with the available power. The glide, instead, must be reduced as the available power and the storage temperature decrease. Since the thermodynamic cycle is equivalent to the ORC's one, analogue considerations can be repeated for the HP mode. Indeed, in this case too: i) the heat transferred into the heat exchangers is proportional to the mass flow rate as well as the needed power for the compression process; ii) the built-in volume ratio determines the magnitude of the under/over-compression losses by varying the glide and the hot source temperature.

5.2 Carnot battery optimal management: application

This paragraph presents the results of the "Optimal global control strategy" application to a possible case study (district heating). The process boundary conditions and the prosumer energy profiles derive from data collected in the thermodynamic laboratory of the University of Liège, during a representative time period of a about a week, which goes from 6 to 14 November. The electric and the thermal demand are the one required by different users inside the building, mainly due to the lightening and the heating. The renewable source consists in photovoltaic solar panels (PV), which are meant to be installed on the building roof, for a surface area equal to 2000 m^2. The solar panel production is simulated by considering the solar irradiance profile of Liège in 2016 (data available from [17]) on a surface oriented with 40 degree slope and -5 degree Azimuth, corresponding to the optimal angulation for the city coordinate. The solar panel efficiency is assumed constant and equal to 25 %. Besides the solar panels characteristic parameters, other parameters that must be chosen for the simulation (as reported in Table 2) are the energy price values and design parameters such as the storage volume and global heat transfer coefficient. The ambient temperature is considered constant and equal to 15 °C.

According to the considered profile (see Figure 5), a variable electric power demand is required during the entire days, with some peaks occurring during the working hours, even up to 200 kW. The PV production instead starts with the daylight to end at the sunset, with peaks in correspondence of the central hours of the day, which, in some moments, lead to an energy surplus production. The thermal demand less variable during the working hours, except for the first working hours when it presents a peak of even 1000 kW.

TABLE 2: SIMULATION'S PARAMETERS.

	Parameter	Value
Variable costs	C_{pur} (€/kWh)	0.15
	C_{sale} (€/kWh)	0.02
	$C_{DH,fee}$ (€/kW)	631
Storage	V_{sto} (m^3)	10
	UA_{sto} (W/K)	5
Solar panels (PV)	Surface (m^2)	2000
	Efficiency (%)	25

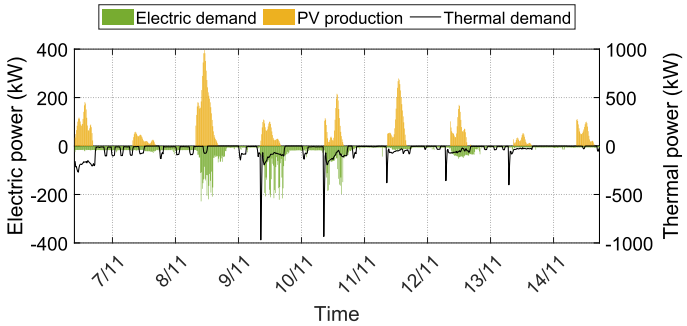

FIGURE 5: PROSUMER ENERGY PROFILES (DATA SAMPLE EVERY 15 MINUTES).

As demonstrative analysis, the results of the code application are presented for a specific scenario, assuming that a free waste heat source provides a constant thermal power of 800 kW. The district heating and the thermal user profiles vary during the day, ranging between 50 °C and 80 °C. Under these boundary conditions, the results of the "Optimal global control strategy" application are shown in figure 6 and Table 3. The energies profile's results prove the convenience in employing the HP to charge the Carnot battery, when possible (for a total of 44 hours):

- in the first five days, the HP allows to store thermal energy to cover the thermal demand peaks of the 9th and 10th of November, opening the possibility of under sizing the DH substation ($\Delta\dot{Q}_{DH,nom}$ results equal to 387 kW), introducing a great economic saving. In these days the ORC is not called to work.
- Being not possible to further undersize the district heating substation, in the following days the HP thermal power production serves instead to increase the storage temperature to enhance the ORC performance. The average ORC efficiency during the operating hours (76) is estimated to be equal to 7 %. The thermal demand is entirely covered by the district heating.

Considering only the week under examination, the differential cost is evaluated equal to 191 €, of which 186 € are associated to the substation under sizing, and 5 € to the self-consumption of the ORC energy production.

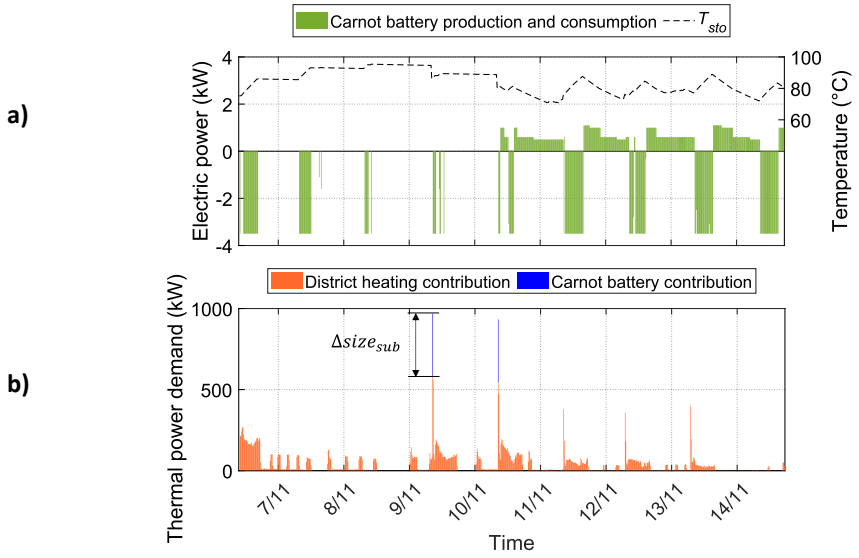

FIGURE 6: ENERGY PROFILES RESULTS: A) ELECTRIC POWER PROFILE; B) THERMAL POWER PROFILE.

TABLE 3: PERFORMANCE INDEXES RESULTS.

	Operating hours	Average η/COP	Production (kWh)	$\Delta size_{sub}$ (kW)	ΔC (€)
HP	44	6	852 (thermal)	387	191
ORC	76	7 %	53 (electric)		

6 CONCLUSION

This paper enriches the current literature on the energy storage topic by proposing a methodology to model the performance of reversible ORC/HP Carnot batteries and its optimal control strategy when inserted into a process. An existing reversible HP/ORC kW-size prototype is considered as reference and its optimal control in both HP and ORC mode under different boundary conditions is assessed. Results of the Carnot battery optimal control strategy application are also presented as demonstrative case study.

Starting from the considerations made, the methodology proposed in this work is meant to be a starting point for further and deeper investigation of the Carnot battery opportunity for residential and industrial applications. In particular, being the methodology established, it is in the Author's intention to systematically explore the influence of crucial parameters (such as the energy costs, size of the panels, the storage and the machines) on the return of the investment for different applications, accounting for an entire year of operation.

REFERENCES

[1] O. Dumont, G. F. Frate, A. Pillai, S. Lecompte, M. De paepe, and V. Lemort, "Carnot battery technology: A state-of-the-art review," *J. Energy Storage*, vol. 32, p. 101756, Dec. 2020, doi: 10.1016/j.est.2020.101756.

[2] O. Dumont and V. Lemort, “Mapping of performance of pumped thermal energy storage (Carnot battery) using waste heat recovery,” *Energy*, vol. 211, p. 118963, Nov. 2020, doi: 10.1016/j.energy.2020.118963.
[3] O. Dumont, A. Léonard, and V. Lemort, “Life cycle analysis of a Carnot battery based on a Rankine cycle (Pumped thermal energy storage), *Proceedings of Ecos conference 2021*.
[4] B. Eppinger, D. Steger, C. Regensburger, J. Karl, E. Schlücker, and S. Will, “Carnot battery: Simulation and design of a reversible heat pump-organic Rankine cycle pilot plant,” *Appl. Energy*, vol. 288, p. 116650, Apr. 2021, doi: 10.1016/j.apenergy.2021.116650.
[5] R. Fan and H. Xi, “Energy, exergy, economic (3E) analysis, optimization and comparison of different Carnot battery systems for energy storage,” *Energy Convers. Manag.*, vol. 252, p. 115037, Jan. 2022, doi: 10.1016/j.enconman.2021.115037.
[6] O. Dumont, S. Quoilin, and V. Lemort, “Experimental investigation of a reversible heat pump/organic Rankine cycle unit designed to be coupled with a passive house to get a Net Zero Energy Building,” *Int. J. Refrig.*, vol. 54, pp. 190–203, Jun. 2015, doi: 10.1016/j.ijrefrig.2015.03.008.
[7] O. Dumont, A. Reyes, and V. Lemort, “Modelling of a thermally integrated Carnot battery using a reversible heat pump/organic Rankine cycle,” presented at the ecos conference, 2020.
[8] O. Dumont, A. Charalampidis, and V. Lemort, “Experimental Investigation Of A Thermally Integrated Carnot Battery Using A Reversible Heat Pump/Organic Rankine Cycle,” *Int. Refrig. Air Cond. Conf.*, May 2021, [Online]. Available: https://docs.lib.purdue.edu/iracc/2085
[9] A. Redko, O. Redko, and R. DiPippo, “9 - Industrial waste heat resources,” in *Low-Temperature Energy Systems with Applications of Renewable Energy*, A. Redko, O. Redko, and R. DiPippo, Eds. Academic Press, 2020, pp. 329–362. doi: 10.1016/B978-0-12-816249-1.00009-1.
[10] O. Dumont, “Investigation of a heat pump reversible into an organic Rankine cycle and its application in the building sector,” PhD Dissertation, 2017.
[11] “Solstice® zd (R-1233zd) | European Refrigerants.” https://www.honeywell-refrigerants.com/europe/product/solstice-zd/ (accessed Aug. 27, 2021).
[12] T. Resimont, “Strategic outline and sizing of district heating networks using a geographic information system,” Université de Liège, Liège, Belgique, 2021. Accessed: Dec. 20, 2021. [Online]. Available: https://orbi.uliege.be/handle/2268/262651
[13] R. Dickes, O. Dumont, R. Daccord, S. Quoilin, and V. Lemort, “Modelling of organic Rankine cycle power systems in off-design conditions: An experimentally-validated comparative study,” *Energy*, vol. 123, pp. 710–727, Mar. 2017, doi: 10.1016/j.energy.2017.01.130.
[14] R. Poskas, *TUBES, SINGLE-PHASE HEAT TRANSFER IN*. Begel House Inc., 2011. doi: 10.1615/AtoZ.t.tubes_single-phase_heat_transfer_in.
[15] V. Lemort, “CONTRIBUTION TO THE CHARACTERIZATION OF SCROLL MACHINES IN COMPRESSOR AND EXPANDER MODES,” University of Liège, 2008.
[16] A. Landelle, N. Tauveron, R. Revellin, P. Haberschill, S. Colasson, and V. Roussel, “Performance investigation of reciprocating pump running with organic fluid for organic Rankine cycle,” *Appl. Therm. Eng.*, vol. 113, pp. 962–969, Feb. 2017, doi: 10.1016/j.applthermaleng.2016.11.096.
[17] “JRC Photovoltaic Geographical Information System (PVGIS) - European Commission.” https://re.jrc.ec.europa.eu/pvg_tools/it/#MR (accessed Dec. 17, 2021).